Food Chemistry 404 (2023) 134546

Contents lists available at ScienceDirect

Food Chemistry

journal homepage: www.elsevier.com/locate/foodchem

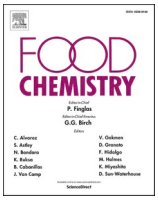

Appraisal of a new potential antioxidants-rich nutraceutical ingredient from chestnut shells through *in-vivo* assays – A targeted metabolomic approach in phenolic compounds

Diana Pinto [a], Andreia Almeida [a], Anallely López-Yerena [b], Soraia Pinto [c,d], Bruno Sarmento [c,d,e], Rosa Lamuela-Raventós [b,f], Anna Vallverdú-Queralt [b,f,*], Cristina Delerue-Matos [a], Francisca Rodrigues [a,*]

[a] *REQUIMTE/LAQV, Instituto Superior de Engenharia do Porto, Rua Dr. António Bernardino de Almeida, 4249-015 Porto, Portugal*
[b] *Nutrition, Food Science and Gastronomy Department, School of Pharmacy and Food Science, University of Barcelona, Barcelona, Spain*
[c] *i3S – Institute for Research and Innovation in Health, University of Porto, Rua Alfredo Allen, 208, 4200-135 Porto, Portugal*
[d] *INEB – Institute of Biomedical Engineering, University of Porto, Rua Alfredo Allen, 208, 4200-135 Porto, Portugal*
[e] *CESPU – Institute for Research and Advanced Training in Health Sciences and Technologies, Rua Central de Gandra 1317, 4585-116 Gandra, Portugal*
[f] *Consorcio CIBER, M.P. Fisiopatología de la Obesidad y la Nutrición (CIBERObn), Instituto de Salud Carlos III (ISCIII), Madrid, Spain*

ARTICLE INFO

Keywords:
Castanea sativa
Subcritical water extraction
Polyphenols
In-vivo study
Nutraceutical
Metabolomic

ABSTRACT

Chestnut (*Castanea sativa*) shells (CSS) are a source of bioactive compounds with well demonstrated *in-vitro* antioxidant properties. Nevertheless, no *in-vivo* studies have already evaluated this effect. This study evaluated the effects of the oral daily administration of an eco-friendly CSS extract (50 and 100 mg/kg per body weight (b.w.)) to rats regarding *in-vivo* antioxidant activity, glucose and lipids levels, and metabolomic profiling of polyphenols by LC-ESI-LTQ-Orbitrap-MS. The results demonstrated the *in-vivo* antioxidant properties in the animals liver, kidney and blood serum, as well as protective effects against hemolysis and rising of blood glucose and lipids levels. New insights on metabolomic profiling of polyphenols proved their absorption and further biotransformation by phase I (hydrogenation and hydroxylation) and II reactions (glucuronidation, methylation and sulfation). This is the first study that attempted to validate a novel nutraceutical ingredient extracted from CSS by *in-vivo* assays, corroborating the outcomes screened by *in-vitro* assays.

1. Introduction

The intake of food supplements and nutraceuticals plays a leading role in the daily diet of society for health-promoting purposes, mainly ascribed to the phytochemical compounds possessing outstanding antioxidant effects. The use of *in-vitro* assays to appraise the antioxidant properties of natural extracts is well-documented, but it is still poorly related to their *in-vivo* bioactivity (Babbar, Oberoi, & Sandhu, 2015; Martins, Barros, & Ferreira, 2016). The assessment of the *in-vivo* antioxidant activity is challenging owing to the complex multiple targets of natural extracts possessing this effect and the limited number of oxidative stress markers (Babbar et al., 2015). Studies in animal models and healthy subjects to ascertain the real *in-vivo* antioxidant activity of isolated phytochemicals and foods are still scarce (Martins et al., 2016). These studies are even fewer for agro-industrial by-products, such as chestnut shells, highlighting a lack in the food research field.

The chestnut industry is a major part of the Portuguese economy owing to its fruits, considered an added-value resource. The shells generated during chestnut processing are an abundant and undervalued by-product, not entirely depleted by their reuse as biomass for energy production (Pinto, Cádiz-Gurrea, Vallverdú-Queralt, et al., 2021). Previous studies have only explored the *in-vitro* bioactivity and phytochemical composition of CSS extracts, mostly prepared by proficient and eco-friendly technologies (Pinto et al., 2020; Pinto, Silva, et al., 2021; Pinto, Vieira, et al., 2021). Recently, Pinto, Vieira, et al. (2021)

* Corresponding authors at: Nutrition, Food Science and Gastronomy Department, School of Pharmacy and Food Science, Av Joan XXIII s/n 08028 Barcelona, University of Barcelona, Barcelona, Spain (A. Vallverdú-Queralt). REQUIMTE/LAQV - Instituto Superior de Engenharia do Porto, Rua Dr. António Bernardino de Almeida, 431, 4249-015 Porto, Portugal (F. Rodrigues).
E-mail addresses: avallverdu@ub.edu (A. Vallverdú-Queralt), francisca.rodrigues@graq.isep.ipp.pt (F. Rodrigues).

https://doi.org/10.1016/j.foodchem.2022.134546
Received 7 August 2022; Received in revised form 17 September 2022; Accepted 5 October 2022
Available online 8 October 2022

optimized the subcritical water extraction (SWE) of CSS through Response Surface Methodology. The optimal extract attained at 220 °C/30 min demonstrated exceptional antioxidant, antiradical, anti-inflammatory, and antimicrobial properties (Pinto, Cádiz-Gurrea, Garcia, et al., 2021; Pinto, Vieira, et al., 2021). Ellagic acid, gallic acid, protocatechuic acid, methyl gallate and pyrogallol were identified as the major polyphenols (Pinto, Vieira, et al., 2021). The food and nutraceutical segments have, therefore, new opportunities to valorize chestnut shells. Recent advances corroborate the promising *in-vivo* bioactivity of other chestnut species. Kimura et al. (2011) and Lee et al. (2022) suggested the use of proanthocyanidins extracted from *Aesculus turbinata* shells and phenolic compounds from *Castanea crenata* inner shells as dietary supplements due to their anti-obesity effects in mice, proven by the inhibition of lipids and carbohydrates digestive enzymes. In another study, the *in-vivo* antioxidant potential of *C. crenata* shells extract in tetrachloromethane and high-fat diet-treated mice was determined, while Noh et al. (2011) reported the hepatoprotective effects of *C. crenata* shells against ethanol-induced oxidative stress.

Metabolomic insights may offer prominent opportunities to ascertain the absorption and distribution of bioactive compounds and their metabolites in different tissues or biological fluids and explain the overall health effects (López-Yerena, Domínguez-López, et al., 2021). The *in-vivo* biological effects of phenolic compounds are determined by their bioavailability, metabolism, intestinal absorption, and interaction with target tissues (López-Yerena, Domínguez-López, et al., 2021; Marhuenda-Muñoz et al., 2019). Beyond the low oral bioavailability, phenolic compounds undergo biotransformation through phase I and II reactions, as well as by the gut microbiota (López-Yerena, Domínguez-López, et al., 2021). Given the broad and promising range of biological activities, most research on chestnut shells has centered on the phenolic compounds' extraction and their *in-vitro* bioactivity (Barreira, Ferreira, Oliveira, & Pereira, 2008; Pinto, Vieira, et al., 2021). Therefore, a deep understanding of the bioavailability of phenolic compounds is vital to disclose the mechanisms behind their bioactivity.

The current study was designed to determine the effects of the daily oral administration of chestnut shells extract prepared by SWE to rats on *in-vivo* antioxidant activity and targeted metabolomic profile of phenolic compounds in blood serum by liquid chromatography coupled to Orbitrap-mass spectrometry (LC-ESI-LTQ-Orbitrap-MS). Blood glucose and lipids levels, as well as histological analyses of liver and kidney were screened. The effect of CSS extract on erythrocytes hemolysis was estimated, while Principal Component Analysis was used to explore the differences between the treatment groups. This is the first study that provides a comprehensive assessment of the *in-vivo* antioxidant activity of nutraceutical extracts from chestnut shells in rat models and explores the relationship to the metabolic fingerprinting of phenolic compounds.

2. Materials and methods

2.1. Chemicals

All chemical reagents were of analytical grade, used as received or dried by standard procedures. Standards used for the metabolomic analysis were acquired as follows: benzoic acid, 2,5-dihydroxybenzoic acid, 2,6-dihydroxybenzoic acid, 3,5-dihydroxybenzoic acid, 3,4-dihydroxyhydrocinnamic acid (or dihydrocaffeic acid, DHCA), 3-(2,4-dihydroxyphenyl)propionic acid, 4-hydroxybenzoic acid (HBA), 3-hydroxyphenylacetic acid, 3-(4-hydroxyphenyl)propionic acid (HPPA), caffeic acid (CA), catechol, chlorogenic acid, cinnamic acid, *o*-coumaric acid, *m*-coumaric acid, ellagic acid, enterodiol, enterolactone, gallic acid, hippuric acid, homovanillic acid, phenylacetic acid, protocatechuic acid, pyrogallol, secoisolariciresinol, sinapic acid, urolithins A and B, vanillic acid, and vanillin from Sigma-Aldrich (Steinhemin, Germany); (-)-epicatechin, 3-HBA, ρ-coumaric acid, ferulic acid (FA) and syringic acid from Fluka (St. Louis, MO, USA); methyl gallate from Phytolab (Vestenbergsgreuth, Germany); and 3-(4-hydroxy-3-methoxyphenyl)propionic acid (or dihydroferulic acid, DHFA) from Alfa Aesar (Haverhill, MA, USA). Acetonitrile, methanol and formic acid were obtained from Sigma-Aldrich (Steinhemin, Germany).

2.2. Castanea sativa shells

Chestnut shells were provided by Sortegel (Sortes, Bragança, Portugal) in October 2018, dehydrated at 40 °C/24 h and ground to 1 mm of particle size using Retsch ZM200 ultra-centrifugal grinder (Germany). Samples were stored in the dark at room temperature.

2.3. Subcritical water extraction of C. sativa shells

SWE was accomplished according to Pinto, Vieira, et al. (2021). Extraction was conducted at 220 °C and 40 bar, for 30 min, using a 400 mL Parr Reactor (Series 4560, Parr Instrument Company, Moline, Illinois, USA) attached to a Parr Reactor Controller (Series 4848). Powdered shells (10 g) were mixed with deionized water (100 mL) and continuous agitation was ensured by a four-blade impeller (200 rpm). The extract was filtered through Whatman n° 1 paper, centrifuged at 8000 rpm for 5 min (Sigma 3-30KS, Sigma, Germany), lyophilised (Telstar, Cryodos −80, Spain) and stored at 4 °C.

2.4. In-vivo studies

2.4.1. Animals and experimental design

Male Wistar rats (200 ± 50 g, 5–6 weeks old), provided by Jackson Laboratory (Bar Harbor, ME, USA), were acclimatized to the animal facility for 1 week prior to the experiments and then housed in polypropylene cages under standard laboratory conditions (temperature: 21 ± 2 °C; relative humidity; 45–55 %; light/dark cycle: 12 h/12 h) and fed *ad libitum* with standard pellet diet and water. Rats were randomly divided into four groups (n = 6 per group): a normal control group administered with water (4 mL/kg body weight (b.w.)); positive control group administered with vitamin C (50 mg/kg b.w.); two treatment groups administered with two doses of CSS extract dispersed in water (50 and 100 mg/kg b.w.). All solutions were administered once daily *p.o.* by gastric gavage for 7 days after 4 h of fasting period. Acute toxicity test was performed using the same two doses of extract (50 and 100 mg/kg b.w.) to determine if there were any toxic effects on animals by monitoring health status, body weight and behavior. A commitment with the 3R's policy of animal research (Replacement, Reduction & Refinement) in using the minimum number of animals across all experiments and promoting the animal welfare was also considered. *In-vivo* procedures were approved by the Local Ethical Committee from the Animal Welfare Body at i3S – Institute for Research & Innovation in Health (ref. BSm_2017_10) and performed under the guidance of FELASA and according to the European Directive 2010/63/EU. The general health status of the animals was monitored, and the humane endpoints were set in the case of any toxic effect on animals and impairment of animal welfare. Blood glucose levels were measured at 1st, 4th, and 7th days using a glucometer (Accu-Chek, Roche® Diabetes Care, Inc., QC, Canada). Animals were euthanized by pentobarbital overdose (50 mg/kg b.w.). Blood samples were collected by cardiac puncture. Serum was separated by centrifugation (2000 *g*, 15 min, 4 °C) and stored at −80 °C. Liver and kidneys were dissected, and tissue homogenates were prepared with 50 mM potassium phosphate (pH 7.0) using T10 basic Ultra-Turrax® (IKA laboratory technology, Staufen, Germany) at 1:5 (*w/v*) ratio, centrifuged for 10 min (20,000 *g*, 4 °C) and supernatants were stored at −80 °C.

2.4.2. In-vivo antioxidant activity

In-vivo antioxidant activity was assessed in blood serum, liver, and kidney supernatants by estimating superoxide dismutase (SOD), catalase (CAT) and glutathione peroxidase (GSH-Px) activities and lipid peroxidation (LPO) through determining malondialdehyde (MDA) levels using

commercial kits (Sigma-Aldrich, Steinheim, Germany). Protein content was assessed by Lowry method.

2.4.3. Inhibition of erythrocyte hemolysis in rat blood

A 20 % erythrocytes suspension in 10 mM phosphate buffer saline (PBS, pH 7.4) was prepared according to Barreira et al. (2008). Briefly, rat erythrocytes were separated from plasma and buffy coat, washed with PBS and centrifuged (1500 *g*, 10 min). The reaction mixture containing 20 % erythrocytes suspension, 200 mM 2,2′-azobis(2-amidinopropane)dihydrochloride (AAPH) solution, and extract was incubated at 37 °C, 30 rpm, for 3 h. Finally, PBS was added to the reaction mixture which was centrifuged (3000 *g*, 10 min) and the absorbance of supernatants measured at 540 nm. Ascorbic acid was used as positive control. The inhibition of erythrocytes hemolysis was determined as follows:

$$Inhibition\ \% = [(A_{AAPH} - A_S)/A_{AAPH}] \times 100$$

where A_{AAPH} is the absorbance of control (without extract) and A_S is the absorbance of sample.

2.4.4. Other biochemical analyses

Serum was used to determine the levels of total cholesterol (TC), high-density and low-density lipoprotein cholesterol (HDL and LDL, respectively) using commercial kits (Sigma-Aldrich, Steinheim, Germany). Triglycerides (TG) were estimated by a commercial kit (Abcam, Cambridge, MA, USA).

2.4.5. Targeted metabolomic studies

2.4.5.1. Sample pre-treatment. Blood serum was handled in a room with light-filter and kept on ice. The clean-up step for protein precipitation was achieved following the procedures from other studies (López-Yerena, Vallverdú-Queralt, et al., 2021; Orrego-Lagarón, Martínez-Huélamo, Vallverdú-Queralt, Lamuela-Raventos, & Escribano-Ferrer, 2015). After thawing and centrifuging (11,000 *g*, 4 °C, 10 min), 100 μL of the upper layer was mixed with ice-cold acetonitrile containing 2 % formic acid in a 1:4 (*v/v*) ratio. Samples were homogenized for 1 min, stored at − 20 °C for 20 min, centrifuged for 10 min (11,000 *g*, 4 °C) and finally 100 μL of organic phase transferred to vials for analysis.

2.4.5.2. LC-ESI-LTQ-Orbitrap-MS analysis. Metabolic profiling was studied using LC-ESI-LTQ-Orbitrap-MS equipment composed of Accela chromatograph (Thermo Scientific, Hemel Hempstead, UK) containing a quaternary pump, a photodiode array detector and a thermostated autosampler coupled to a LTQ Orbitrap Velos mass spectrometer (Thermo Scientific, Hemel Hempstead, UK) equipped with an ESI source in negative mode. Samples were examined in full scan mode at a resolving power of 30,000 at *m/z* 600 and data-dependent MS/MS events were acquired at a resolving power of 15,000. Most intense ions were detected in FTMS mode triggered data-dependent scanning. Ions not sufficiently intense for a data-dependent scan were explored in MS^n mode. Precursors were fragmented by collision-induced dissociation using a C-trap with normalized collision energy (35 V) and activation time of 10 ms. Mass range in FTMS mode was from *m/z* 100 to 600. The chromatographic elution was performed using Acquity™ UPLC® BEH C_{18} Column (2.1 × 100 mm, i.d., 1.7 μm particle size) (Waters Corporation, Ireland). The mobile phases were water with 0.1 % formic acid (A) and acetonitrile with 0.1 % formic acid (B). The solvent gradient (*v/v*) of B (t (min), %B) was defined as follows: (0, 0); (2, 0); (3, 30); (4, 100); (5, 100); (6, 0); (9, 0). Injection volume, flow rate and column temperature were set at 5 μL, 0.450 mL/min and 30 °C, respectively.

The instrumental conditions were established as validated by Escobar-Avello et al. (2021) with minor modifications. The identification of phenolic compounds was accomplished using commercial standards, while the identification of metabolites was achieved considering chromatographic elution time, chemical composition, MS/MS fragmentation and comparing with a similar compound. Literature data and human metabolome database (https://hmdb.ca) were consulted as useful tools for the putative identification of the phenolic compounds and metabolites in the blood serum. Regarding the extract, the remaining compounds (of which the standards were not available) were identified by comparison with previous data from our research group (Escobar-Avello et al., 2021; Sasot et al., 2017) regarding retention times, chemical formula and mass spectrometry fragmentation patterns, and confirmed using databases, namely food database (https://foodb.ca) and phenol database (http://phenol-explorer.eu). Similar procedures for the identification of the phenolic compounds in foods and extracts were followed in previous studies (Escobar-Avello et al., 2021; Sasot et al., 2017). MS^n measurements were performed to acquire information about fragment ions generated in the linear ion trap within the same analysis. Accurate masses and isotopic patterns were used to select the elemental composition of metabolites. For quantification purposes, calibration curves (concentration range = 0.1–3 μg/mL, $R^2 > 0.994$) were prepared in blood serum with gallic, ellagic, and protocatechuic acids, pyrogallol and methyl gallate that were previously identified as major polyphenols in the CSS extract (Pinto, Vieira, et al., 2021). Semi-quantification was provided for the remaining phenolic compounds. XCalibur 3.0 software (ThermoFisher Scientific, Hemel Hempstead, UK) was used to control the system and for data treatment. Results were calculated using the peak area of the parent molecule and presented in nmol of each phenolic compound equivalents per mL of serum.

2.4.6. Histological analysis

Tissues were washed with PBS 1 × for 5 min, fixed using 2 % paraformaldehyde for 20 min, and embedded in paraffin. Sections (2–3 mm thickness) were obtained by RM2255 microtome (Leica). After deparaffinizing and rehydrating, sections were stained by a hematoxylin-eosin staining. Briefly, sections were stained in Gil's Hematoxylin (Thermo Scientific) during 3 min, washed for 6 min, dehydrated, and stained in Eosin Y (Thermo Scientific) during 1 min. Stained sections were arranged in Entellan (Merck). Representative photomicrographs of liver and kidney were obtained using Light microscope Olympus DP 25 Camera Software Cell B at 10 × objective magnification.

2.5. Statistical analysis

Results were expressed as mean ± standard deviation of at least three independent experiments. IBM SPSS Statistics 24.0 software (SPSS Inc., Chicago, IL, USA) was used for data statistical analysis. One-way ANOVA was employed to investigate the differences between samples and Tukey's HSD test was used for *post hoc* comparisons of the means. Statistically significant results were denoted for $p < 0.05$. Principal component analysis (PCA) was performed using GraphPad Prism v9 software (La Jolla, CA, USA) to allow the identification of variables that most significantly affect the samples clustering. Two principal components (PC) were used to establish the model after confirming the normal distribution of the variables. A scores plot was designed to identify the trends among treatment groups, while a biplot diagram was used to disclose the contribution of different variables.

3. Results and discussion

3.1. Body weight and blood glucose levels

During the experiments, no phenotypic or behavioral changes were observed in animals. The acute toxicity test also revealed no changes in the general health status, behavior, and body weight for the two extract doses tested (50 and 100 mg/kg b.w.), suggesting the safety of both extract doses in rats. The animals responded well to the procedures applied, maintaining the appropriate body weight to their age and development stage, and the social interaction, without phenotypic and behavioral variations. The body weight was monitored to enlighten

possible impacts of oral administration of CSS extract in the rats' weight. According to Supplementary Fig. S1A, the body weight increased steadily by almost 15 % up to day 7 for control and treatment groups, corresponding to the expected growth rate of 6-week-old rats. Even though the animals treated with CSS extract at 50 and 100 mg/kg b.w. displayed slightly lower body weights than the ones treated with vitamin C and water (control group), there are no significant differences ($p > 0.05$) between groups for any of the days. Soussi, Gargouri, Akrouti, and El Feki (2018) also reported body weights around 210 g for 11–12 weeks old Wistar rats after 5 days of oral treatment with 900 mg/kg b.w. walnut (*Juglans regia*) oil.

The blood glucose levels were monitored at days 1, 4 and 7 (Supplementary Fig. S1B). A mild decrease on blood glucose levels was noticed for rats treated with CSS extract and vitamin C. Almost 20 % and 33 % of reduction was detected in the glucose levels of rats treated with CSS extract at 50 and 100 mg/kg b.w., respectively, while the glucose levels of vitamin C-treated rats decreased 45 %. Significant differences ($p < 0.05$) were observed between days 1 and 7 for the groups treated with 100 mg/kg b.w. CSS extract and vitamin C. Oppositely, the glucose levels of the control group maintained ($p > 0.05$) throughout the 7 days. The results suggested a mild hypoglycemic effect for the CSS extract at 100 mg/kg b.w. Noteworthy, chestnut shells are interesting feedstocks of phenolic compounds and polysaccharides, which play an active role as hypoglycemic compounds (Pinto, Cádiz-Gurrea, Vallverdú-Queralt, et al., 2021). Kimura et al. (2011) studied the anti-obesity effects of proanthocyanidins extracted from Japanese horse chestnut shells, achieving similar blood glucose levels (≈50–200 mg/dL) in mice treated orally with different doses of proanthocyanidins (250–1500 mg/kg b.w.) after starch and glucose (2 g/kg mouse). In an *in-vitro* study, Pinto, Silva, et al. (2021) suggested the hypoglycemic potential of CSS extract with 15 % α-amylase inhibition. Moreover, Tsujita, Takaku, and Suzuki (2008) attested the *in-vivo* anti-hyperglycemic properties of chestnut shells ethanolic extract after oral administration (2 g/kg b.w.) to rats fed corn starch, by preventing the rise of blood glucose levels and modulating α-amylase activity. This effect was attributed to the phenolic composition (67 % polyphenols, 57 % flavanol-type tannins and 51 % procyanidins), mainly to gallic and ellagic acids.

Liver and kidney weights ranged between 4.5 g/100 g b.w. and 0.8 g/100 g b.w., respectively (Supplementary Fig. S1C). No significant differences ($p > 0.05$) were detected between control and treatment groups. Likewise, Kimura et al. (2011) reported similar organ weights for mice fed standard chow diet (control) and high-fat diets with 0.26 % and 0.52 % of proanthocyanidins from *A. turbinata* shells (0.70–1.18 and 3.04–3.89 g/100 g b.w. for kidney and liver, respectively).

3.2. Blood lipids levels

The effects of CSS extract in the blood lipids levels, including TG, HDL, LDL and TC, are presented in Fig. 1.

The highest TG levels were determined in the rats from control group (274.74 mg/dL), while vitamin C and CSS extract 50 mg/kg b.w. induced a slight decrease on TG levels (≈210 mg/dL) (Fig. 1A). Nevertheless, no significant differences ($p > 0.05$) were observed between the control, the vitamin C and the 50 mg/kg b.w CSS extract group. A more noticeable decrease ($p < 0.05$) was observed in rats orally administered with CSS extract 100 mg/kg b.w. (177.29 mg/dL) compared to the control, suggesting a mild hypolipidemic effect. Similar results were reported in mice treated with *C. crenata* inner shells extract

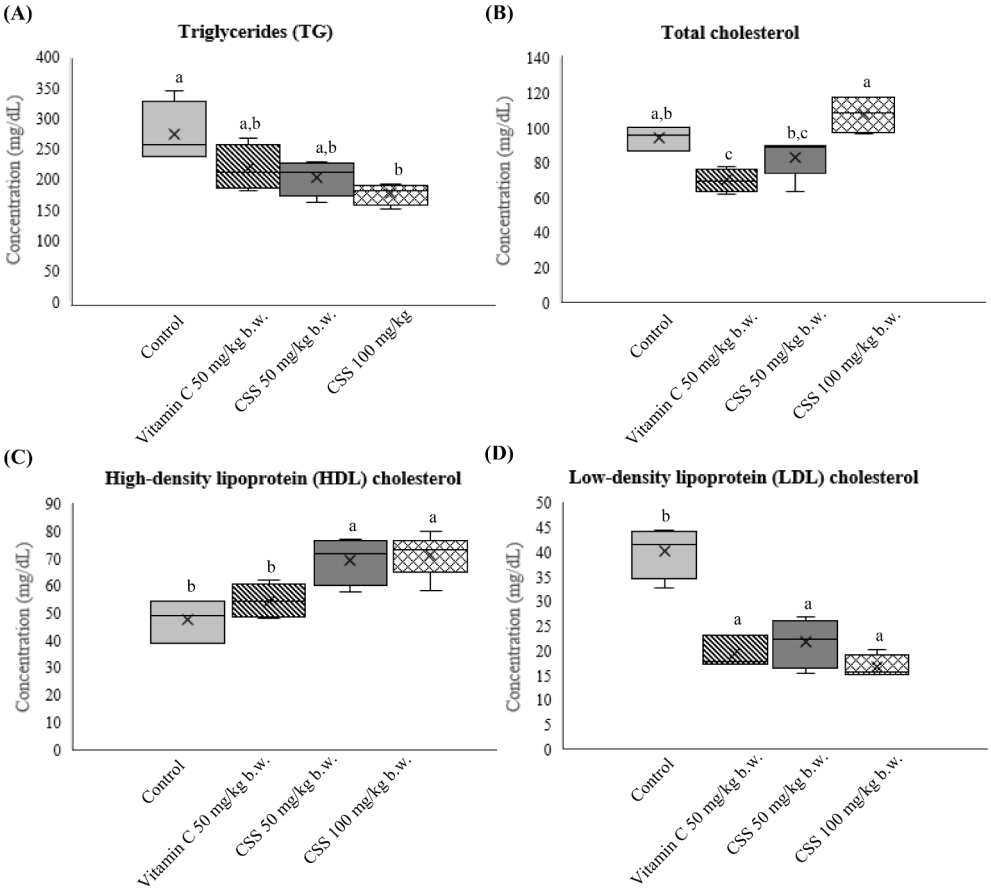

Fig. 1. Lipid levels in blood serum collected from rats treated with *C. sativa* shells extract ($n = 6$). (A) triglycerides (TG), (B) total cholesterol, (C) high-density lipoprotein (HDL) cholesterol, and (D) low-density lipoprotein (LDL) cholesterol. Different letters (a, b and c) indicate significant differences between groups ($p < 0.05$).

prepared by ultrasound-assisted extraction (UAE) (≈100–150 mg/dL) to revert the negative impacts of a high-fat diet (Lee et al., 2022). In addition, Noh et al. (2011) demonstrated the potential of chestnut inner shells extract on the reduction of TG levels (73.7 mg/dL) in C57BL/6 mice administered orally with ethanol compared to mice fed normal standard diet and standard diet plus ethanol (122.4 and 136.0 mg/dL, respectively).

HDL is a key player in several diseases owing to its atheroprotective effect. The health benefits associated to HDL are mainly related to its ability to efflux cholesterol and other lipids from peripheral tissues, such as blood, and transport them to liver for disposal, reducing the risk of cardiovascular diseases (Sirtori & Fumagalli, 2006). Beyond cholesterol-carrying action, HDL is recognized as a multifaceted molecule with complex and not entirely understood physiological functions. Compared to the control, the HLD levels increased 46 % and 50 % ($p < 0.05$) after treatment with the CSS extract at 50 and 100 mg/kg b.w., respectively (Fig. 1C). The HDL levels of the rats treated with vitamin C (54.71 mg/dL) were in line with the ones achieved for the control group (47.64 mg/dL). The present results are slightly lower than the ones reported by Kimura et al. (2011) for mice fed high-fat diets for 19 weeks and treated with 0.26 % and 0.52 % of proanthocyanidins from *A. turbinata* shells (95.8 and 64.8 mg/dL, respectively).

LDL is highly atherogenic and a major risk factor of atherosclerosis. Previous studies confirmed the causal role of high circulating LDL levels in cardiovascular disease risk. Oppositely, lowering LDL reduces the risk of coronary artery disease, myocardial infarction, and ischemic stroke (Sirtori & Fumagalli, 2006). In contrast to HDL, CSS extract-treated rats revealed the lowest LDL levels, with 23.89 and 18.77 mg/dL for 50 and 100 mg/kg b.w., respectively (Fig. 1D). All groups showed significantly reduced LDL levels ($p < 0.05$) compared to the control (40.14 mg/dL).

The TC concentrations increased in the following order: vitamin C (70.07 mg/dL) < 50 mg/kg b.w. CSS extract (83.45 mg/dL) < control (94.56 mg/dL) < 100 mg/kg b.w. CSS extract (98.22 mg/dL) (Fig. 1B). Only vitamin C achieved significantly different results ($p < 0.05$) from control. The outcomes were in agreement with those reported in mice orally treated with proanthocyanidins-rich extract from *A. turbinata* shells to prevent hypercholesteremic effects of a high-fat diet (120.2 and 83.2 mg/dL at 0.26 % and 0.52 % of extract, respectively), proposing its use as an active ingredient for nutraceuticals (Kimura et al., 2011). Although CSS extract-treated rats evidenced similar TC concentrations to control, treatment groups also revealed higher HDL and lower LDL levels, which possibly suggests better atheroprotective effects and lower cardiovascular risk after oral treatment with CSS extract. Another study revealed that *C. crenata* shells extract reduces obesity and intramuscular lipid accumulation due to its wealth in gallic and caffeic acids (Lee et al., 2022). Indeed, phenolic compounds may protect against LDL oxidation, enhance HDL profile and improve antioxidant and anti-inflammatory properties (Sirtori & Fumagalli, 2006). Overall, CSS extract may be considered as a potential candidate for monitoring high blood cholesterol levels, with preventive effects from cardiovascular pathologies, owing to its richness in phenolic compounds.

3.3. *In-vivo* antioxidant effects

The *in-vivo* antioxidant activity of blood serum, liver and kidney homogenates from rats orally treated with CSS extract is summarized in Table 1.

In liver, GSH-Px activity enhanced 61 % ($p < 0.05$) from 50 to 100 mg/kg b.w. of CSS extract, respectively, while SOD activity only increased 10 % ($p > 0.05$). Comparing to the control group, the CSS extract treated rats displayed an augment ($p < 0.05$) of 29 % and 41 % in the SOD activity, respectively, at 50 and 100 mg/kg b.w., while the GSH-Px activity was 2-fold and 3-fold higher ($p < 0.05$) after oral treatment with 50 and 100 mg/kg b.w. extracts, respectively. The MDA content significantly decreased ($p < 0.05$) with the increase of the extract dose from 50 to 100 mg/kg b.w.. Additionally, rats treated with both doses of CSS extract presented substantially lower LPO ($p < 0.05$) than those administered with water (control) and vitamin C. Otherwise, the CAT activity remained almost unchanged, presenting a slightly higher result in the control. Both CSS extract groups demonstrated similar CAT activity ($p > 0.05$). Noh et al. (2010) attested the *in-vivo* antioxidant activity in liver of mice orally treated with 150 mg/kg b.w. *C. crenata* shells extract and 1 mg/kg b.w. tetrachloromethane administered intraperitoneally as oxidative stress inductor, revealing similar CAT (≈7–10 U/mg protein), SOD (≈500–1500 U/g protein) and GSH-Px activities (≈120–140 U/g protein), reporting better results in extract-treated mice. Furthermore, a significant reduction in LPO was detected after oral treatment with chestnut shells extract. Nevertheless, these authors tested a higher dose of extract comparatively to the present study (100 mg/kg b.w.) and demonstrated identical *in-vivo* antioxidant effects.

Considering kidney, the SOD activity improved 14 % ($p < 0.05$) from 50 to 100 mg/kg b.w. of CSS extract, respectively, while the CAT activity reduced 92 % ($p < 0.05$) from 50 to 100 mg/kg b.w. of CSS extract. Compared to the control, the SOD activity boosted 26 % and 44 %, respectively, in 50 and 100 mg/kg b.w. CSS extract groups ($p < 0.05$). Although the CAT activity of rats treated with 50 mg/kg b.w. CSS extract was significantly higher ($p < 0.05$) than the control, no significant differences ($p > 0.05$) were observed between the 100 mg/kg b.w. CSS extract and the control. The GSH-Px activity of the CSS extract treated rats was twice higher ($p < 0.05$) than the control. The LPO decreased in the following order: control > vitamin C > 50 mg/kg b.w. CSS extract > 100 mg/kg b.w. CSS extract. Significant differences ($p < 0.05$) in the MDA content were found between the CSS extract and the control

Table 1
In-vivo effects on antioxidant enzymes activities, namely superoxidase dismutase (SOD), catalase (CAT) and glutathione peroxidase (GSH-Px), and lipid peroxidation (LPO) in liver, kidney and blood serum from rats treated with *C. sativa* shells extract ($n = 6$).

	Groups			
	CSS extract 50 mg/kg b.w.	CSS extract 100 mg/kg b.w.	Vitamin C 50 mg/kg b.w.	Control
Liver				
SOD (U/g protein)	531.78 ± 81.78^{a}	582.15 ± 65.52^{a}	386.37 ± 56.64^{b}	413.09 ± 102.53^{b}
CAT (U/mg protein)	12.56 ± 1.45^{b}	12.08 ± 1.38^{b}	8.89 ± 1.42^{c}	17.19 ± 2.86^{a}
GSH-Px (U/g protein)	157.61 ± 45.68^{b}	253.28 ± 40.18^{a}	156.92 ± 25.71^{b}	77.11 ± 1.45^{c}
LPO (nmol MDA/mg protein)	2.32 ± 0.25^{c}	1.14 ± 0.07^{d}	5.39 ± 0.35^{b}	6.46 ± 0.62^{a}
Kidney				
SOD (U/g protein)	725.75 ± 41.74^{a}	825.99 ± 94.27^{b}	606.13 ± 37.04^{c}	575.53 ± 46.59^{c}
CAT (U/mg protein)	5.14 ± 0.13^{a}	2.68 ± 0.25^{b}	2.27 ± 0.24^{c}	2.34 ± 0.45^{b,c}
GSH-Px (U/g protein)	316.84 ± 49.71^{a}	327.15 ± 48.92^{a}	216.19 ± 35.92^{b}	134.22 ± 27.15^{c}
LPO (nmol MDA/mg protein)	3.40 ± 0.68^{b}	1.96 ± 0.30^{b}	7.49 ± 1.18^{a}	8.76 ± 1.34^{a}
Blood serum				
SOD (U/g protein)	148.03 ± 19.43^{a}	126.79 ± 13.45^{a,b}	120.10 ± 18.93^{b}	109.24 ± 6.73^{b}
CAT (U/g protein)	25.31 ± 3.75^{b}	26.19 ± 2.53^{b,a}	25.19 ± 5.91^{b}	31.35 ± 2.92^{a}
GSH-Px (U/g protein)	25.61 ± 7.24^{b,c}	64.97 ± 13.38^{a}	34.32 ± 2.89^{b}	23.00 ± 7.67^{c}
LPO (nmol MDA/mg protein)	17.83 ± 2.12^{a}	7.58 ± 1.50^{b}	8.68 ± 1.44^{b}	16.22 ± 2.73^{a}

Results are expressed as mean ± standard deviation, $n = 6$ in each group. Different letters (a, b, c) in the same line indicate significant differences between groups ($p < 0.05$).

groups. Soussi et al. (2018) reported higher SOD and CAT activities in kidneys from walnut oil-treated rats. However, similar MDA contents were determined (2–4 nmol MDA/mg protein). Notwithstanding, the dose of walnut oil tested was 9 times higher (900 mg/kg b.w.) than the CSS extract employed in this study, which may explain the higher antioxidant enzymes' activities.

In the blood serum, the SOD activity enhanced 36 % and 16 % in rats treated with 50 and 100 mg/kg b.w. CSS extract, respectively, when compared to the control. The GSH-Px activity of the 100 mg/kg b.w. CSS extract-treated rats was almost three times higher than the control, while the LPO of 100 mg/kg b.w. CSS extract group was 2-fold lower than the control. Otherwise, the GSH-Px activity and the MDA content of the 50 mg/kg b.w. CSS extract group were similar to the control. The CAT activity remained almost unchanged, with slightly better results in the control. Only rats treated with the lowest dose of CSS extract (50 mg/kg b.w.) displayed significantly different ($p < 0.05$) SOD and CAT results compared to the control, while significantly different GSH-Px and LPO results were only attained for the highest dose of CSS extract (100 mg/kg b.w.). No significant differences ($p > 0.05$) in SOD and CAT activities were observed between the CSS extract groups. Hong, Groven, Marx, Rasmussen, and Beidler (2018) appraised the antioxidant effects of mixed nuts (including almonds, Brazil nuts, cashews, macadamia nuts, peanuts, pecans, pistachios, and walnuts) in rats under standard diet without nuts (control), diet with 8.1 % pistachio (single-nut diet), and 7.5 % of mixed nuts diet (mixed-nuts diet) for 8 weeks. Only mixed-nuts diet induced significantly higher SOD (55 U/mL) and CAT (80 nmol/min/mL) activities when compared to the control diet (SOD = 48 U/mL; CAT = 110 nmol/min/mL), while the GSH-Px activity was identical.

Vitamin C is a powerful water-soluble antioxidant. The dose 50 mg/kg b.w. was selected based on previous studies attesting the efficacy of vitamin C as antioxidant, providing protection from oxidative stress-mediated damages through scavenging reactive species, neutralizing lipid hydroperoxyl radicals and preventing protein alkylation (Traber & Stevens, 2011). For this reason, vitamin C was orally administered to rats as positive control to elucidate about the *in-vivo* effects of a well-known antioxidant on endogenous antioxidant enzymes' activities and prevention of LPO damages. In liver and kidney, both doses of CSS extract induced significantly better antioxidant activity *in-vivo* comparatively to rats treated with water (control) and vitamin C, by upmodulating all antioxidant enzymes' activities and downmodulating lipid peroxidation, as attested by significant differences ($p < 0.05$). In blood serum, only the dose of 50 mg/kg b.w. of CSS extract induced a significant upgrade ($p < 0.05$) on SOD activity, while a substantially improved GSH-Px activity was detected in rats treated with 100 mg/kg b.w. CSS extract. Otherwise, vitamin C and both doses of CSS extract prompted similar effects on CAT activity and LPO.

Particularly, liver and kidney tissues demonstrated higher *in-vivo* antioxidant properties by effectively upregulating CAT, SOD and GSH-Px activities and downregulating LPO, followed by blood serum. Liver is one of the main metabolic organs, being implicated in the metabolism of macronutrients (such as carbohydrates, proteins, and fat) and micronutrients, including phenolic compounds (Liu, Wang, Liang, & Roberts, 2017). Although kidney is primarily responsible for osmoregulation, regulation of acid-base balance, reabsorption of nutrients and excretion, this organ also plays a key role in metabolism, being mainly involved in phase II reactions (Tian & Liang, 2021). A possible explanation for the better results in liver and kidney may be related with the higher accumulation of phenolic compounds and their metabolites, which have been described as potentially more biologically active than the parent compounds that originated them, contributing to a marked antioxidant activity *in-vivo* (Eseberri et al., 2022; Marhuenda-Muñoz et al., 2019). Overall, the results indicated that CSS extract obtained by SWE strongly inhibited rat aging. Noteworthy, similar or even better *in-vivo* antioxidant effects were outlined in rats treated with CSS extract 100 mg/kg b.w. comparatively to 50 mg/kg b.w., confirming the highest dose of extract induced moderately better antioxidant responses in rats.

3.4. Inhibition of erythrocyte hemolysis

Erythrocyte hemolysis is the consequence of cells oxidative injuries caused by free radicals, such as peroxyl radicals produced by AAPH (Barreira et al., 2008). Supplementary Figure S2 represents the inhibitory potential of CSS extract and vitamin C against erythrocyte hemolysis. As shown in the figure, the CSS extract efficiently inhibited the erythrocytes hemolysis by protecting their membranes against oxidative damages induced by AAPH, following a concentration-dependent manner, with values ranging between 45.01 % (31.25 μg/mL) and 67.26 % (1000 μg/mL). The IC_{50} value was 34.71 μg/mL. Likewise, vitamin C achieved similar inhibitory effects on hemolysis, with 55.31 % (31.25 μg/mL) and 72.23 % (1000 μg/mL). No significant differences ($p > 0.05$) were noticed between most concentrations of CSS extract and vitamin C, except for 31.25 μg/mL ($p < 0.05$). These results were better than the ones reported for chestnut inner and outer shells, with IC_{50} values of 47.5 and 91.4 μg/mL, respectively (Barreira et al., 2008). Additionally, *Pinus koraiensis* seeds extract prepared by UAE displayed 50 % of inhibition at 0.04 mg/mL, while vitamin C led to 60 % of inhibition at the same concentration (Su, Wang, & Liu, 2009). Therefore, the results showed a highly protective effect of the CSS extract against injuries on erythrocytes membranes.

3.5. Metabolomic profiling of chestnut shells extract in blood serum

In our previous study, gallic acid, ellagic acid, protocatechuic acid, pyrogallol and methyl gallate were identified as the major phenolic compounds in CSS extract prepared using the same extraction technology and conditions (Pinto, Vieira, et al., 2021). Nevertheless, some unknown compounds were also detected. Notwithstanding, an in-depth and comprehensive analysis of the CSS extract was performed to identify the unknown compounds prior to the metabolomic approach in blood serum (Supplementary Table S1). Beyond the phenolic compounds identified in the previous team work (Pinto, Vieira, et al., 2021), the remaining parent compounds of all metabolites identified in blood serum were detected in the CSS extract. In addition, other phenolic compounds were also noticed, including CA-*O*-hexoside, coumaric acid-*O*-hexoside, coumaroylquinic acid, dicaffeoylquinic acid, (*epi*)catechin-*O*-gallate, (*epi*)catechin-*O*-hexoside, (*epi*)gallocatechin, (*epi*)gallocatechin gallate, FA-*O*-hexoside, feruloylquinic acid, hydroxybenzoyl-*O*-hexoside, sinapic acid-*O*-hexoside, and syringic acid-*O*-hexoside, which can lose either glucose, gallic or quinic acid moieties during metabolism (Sasot et al., 2017), originating the parent compounds and their metabolites (Eseberri et al., 2022). For instance, CA-*O*-hexoside was probably metabolized into CA, which was further converted to other metabolites. The same applies to the other phenolic glycosides detected. Similar phenolic profiles were also reported by Pinto et al. (2020) and Sangiovanni et al. (2018) in eco-friendly chestnut shells extracts.

3.5.1. Identification of phenolic compounds and metabolites

Phenolic compounds undergo biotransformation, including phase I (hydrolysis, oxidation, and reduction) and II (glucuronidation, methylation and sulfation) reactions, generally leading to stabilization and increasing the water solubility and, therefore, modifying their distribution and excretion (López-Yerena, Domínguez-López, et al., 2021; Pimpão, Ventura, Ferreira, Williamson, & Santos, 2015). These reactions may deliver phenolic metabolites equally or more biologically active than the parent compounds that originate them (Eseberri et al., 2022; Marhuenda-Muñoz et al., 2019). Noteworthy, this is the first study that evaluated the metabolomic profile of phenolic compounds in rat blood serum after oral treatment with CSS extract. Table 2 presents the phenolic compounds and the metabolites identified in the blood serum, producing a total of 52 identified compounds.

Most of the phenolic compounds identified are phenolic acids and

Table 2
Identification of phenolic compounds and metabolites in blood serum from rats treated with *C. sativa* shells extract by LC-ESI-LTQ-Orbitrap-MS.

Compound	Neutral molecular formula	Rt (min)	Ion mass [M−H]⁻		Error (ppm)	MS^2 fragment ions [M−H]⁻
			Theoretical	*Experimental*		
Methyl-pyrogallol-*O*-sulfate	$C_7H_8O_6S$	0.73	218.9958	218.9967	0.336	125.02416, 138.97908
Dihydrogallic acid	$C_7H_8O_5$	0.74	171.0288	171.0265	−2.828	127.03718, 141.01816
Protocatechuic acid-*O*-sulfate	$C_7H_6O_7S$	4.34	232.9751	232.9756	0.012	109.02917, 153.01849, 188.98633
Dimethyl-pyrogallol-*O*-glucuronide	$C_{14}H_{18}O_9$	4.44	329.0867	329.0870	−0.247	125.02511, 139.03949, 153.01916
Catechol-*O*-sulfate	$C_6H_6O_5S$	4.47	188.9852	188.9860	0.800	109.02921
Protocatechuic acid*	$C_7H_6O_4$	4.48	153.0182	153.0192	0.366	109.02860, 125.02344
Urolithin A-*O*-sulfate	$C_{13}H_8O_7S$	4.50	306.9907	306.9909	−0.308	227.03806
Pyrogallol-*O*-sulfate	$C_6H_6O_6S$	4.53	204.9801	204.9806	−0.083	123.00834, 125.02385, 162.96728
Hydroxybenzoic acid-*O*-sulfate	$C_7H_6O_6S$	4.56	216.9801	216.9798	−0.903	121.02944, 137.02446
Dimethyl-pyrogallol-*O*-sulfate	$C_8H_{10}O_6S$	4.59	233.0114	233.0121	0.146	125.02511, 139.03949,153.01931, 204.98111
Methyl-protocatechuic acid-*O*-sulfate	$C_8H_8O_7S$	4.62	246.9907	246.9914	0.192	109.02931, 153.01921, 167.03576, 232.97561
Dihydrocaffeic acid-*O*-sulfate	$C_9H_{10}O_7S$	4.64	261.0064	261.0071	0.790	113.06058, 137.06062, 181.05060
Pyrogallol-*O*-glucuronide	$C_{12}H_{14}O_9$	4.65	301.0554	301.0591	3.163	125.02433
Methyl-syringic acid-*O*-sulfate	$C_{10}H_{12}O_8S$	4.66	291.0169	291.0178	0.287	137.06066, 197.04301, 211.06108
Methyl-catechol	$C_{12}H_{14}O_8$	4.68	123.0441	123.0448	0.754	109.02926
Hydroxychlorogenic acid	$C_{16}H_{18}O_{10}$	4.69	369.0816	369.0823	0.647	207.01223
Methyl-protocatechuic acid	$C_8H_8O_4$	4.69	167.0339	167.0348	0.366	109.02923, 153.01918
Caffeic acid-*O*-sulfate	$C_9H_8O_7S$	4.69	258.9907	258.9920	0.850	135.04504, 179.03489, 215.00110
Dihydroferulic acid-*O*-glucuronide	$C_{16}H_{20}O_{10}$	4.70	371.0973	371.0979	0.597	151.03982, 195.06628
Hydroxyphenylacetic acid-*O*-sulfate	$C_8H_8O_6S$	4.72	230.9958	230.9965	0.665	107.05001, 151.03999, 187.00711, 213.00527
Dimethyl-syringic acid-*O*-sulfate	$C_{11}H_{14}O_8S$	4.75	305.0326	305.0330	0.426	153.05548, 197.04302, 225.07685,277.00170
Catechol-*O*-glucuronide	$C_{12}H_{14}O_8$	4.77	285.0605	285.0608	0.286	109.02917
Methyl-ferulic acid-*O*-glucuronide	$C_{17}H_{20}O_{10}$	4.82	383.0973	383.0982	0.947	163.02670, 174.98718, 193.05078, 207.05070, 369.08253
Dihydroferulic acid-*O*-sulfate	$C_{10}H_{12}O_7S$	4.84	275.0220	275.0229	0.850	195.06596
Hydroxyphenylpropionic acid-*O*-sulfate	$C_9H_{10}O_6S$	4.86	245.0114	245.0122	0.795	121.02935, 165.05573, 201.07681
Methyl-coumaric acid-*O*-sulfate	$C_{10}H_{10}O_6S$	4.87	257.0114	257.0158	4.405	119.04989, 163.03987, 177.05564, 199.00630
Methyl-catechol-*O*-sulfate	$C_7H_8O_5S$	4.88	203.0009	203.0018	0.879	123.04492
Dihydrocaffeic acid*	$C_9H_{10}O_4$	4.89	181.0495	181.0505	0.366	109.04048, 137.06017
Hippuric acid*	$C_9H_9NO_3$	4.92	178.0499	178.0506	0.172	134.06059
Syringic acid*	$C_9H_{10}O_5$	4.95	197.0444	197.0451	0.072	137.02383, 153.05535
Ellagic acid*	$C_{14}H_6O_8$	4.96	300.9979	300.9981	−0.372	201.01796, 229.01404, 257.00763, 283.99559
Methyl-dihydroferulic acid-*O*-sulfate	$C_{11}H_{14}O_7S$	4.97	289.0376	289.0384	−1.792	151.07650, 165.01923, 195.06564, 209.08016
3-Hydroxybenzoic acid*	$C_7H_6O_3$	4.98	137.0233	137.0242	0.321	93.03386
Hydroxyphenylpropionic acid*	$C_9H_{10}O_3$	5.05	165.0546	165.0553	0.171	121.02926
Hydroxyferulic acid	$C_{10}H_{10}O_5$	5.06	209.0444	209.0455	1.030	133.99126, 149.02384, 165.05574, 178.05046
Methyl-syringic acid	$C_{10}H_{12}O_5$	5.06	211.0601	211.0611	0.462	137.06030, 153.05548, 197.04174
ρ-Coumaric acid*	$C_9H_8O_3$	5.07	163.0390	163.0399	0.351	119.04975
Dimethyl-hydroxyphenylpropionic acid-*O*-sulfate	$C_{11}H_{14}O_6S$	5.07	273.0427	273.0434	0.675	121.02919, 165.05538, 193.08687
(*Epi*)catechin-*O*-sulfate	$C_{15}H_{14}O_9S$	5.07	369.0275	369.0269	−0.629	245.01231, 289.07153, 303.01690
Cinnamic acid-*O*-glucuronide	$C_{15}H_{16}O_8$	5.09	323.0761	323.0770	0.806	147.04501
Dihydroferulic acid*	$C_{10}H_{12}O_4$	5.10	195.0652	195.0662	0.426	135.04459, 151.07562
Dimethyl-ellagic acid	$C_{16}H_{10}O_8$	5.11	329.0292	329.0275	−2.292	113.06061, 174.98718, 300.99997
Methyl-ferulic acid-*O*-sulfate	$C_{11}H_{12}O_7S$	5.13	287.0220	287.0224	0.430	149.06051, 193.05064, 207.06135, 273.00712
Dihydrocaffeic acid-*O*-glucuronide	$C_{15}H_{18}O_{10}$	5.14	357.0816	357.0823	0.717	113.06061, 137.06066, 174.98715, 181.05055
m-Coumaric acid*	$C_9H_8O_3$	5.15	163.0390	163.0398	0.301	119.04967
Sinapic acid-*O*-sulfate	$C_{11}H_{12}O_8S$	5.15	303.0169	303.0168	−0.074	223.06104
Secoisolariciresinol*	$C_{20}H_{26}O_6$	5.16	361.1648	361.1649	−0.183	165.05508, 346.14081
Hydroxyphenylacetic acid-*O*-glucuronide	$C_{14}H_{16}O_9$	5.26	327.0711	327.0717	0.652	151.03983, 175.02472, 309.05656
Enterolactone-*O*-disulfate	$C_{18}H_{18}O_{10}S_2$	5.32	457.0258	457.0262	−0.123	297.11398, 377.06977
Methyl-urolithin A	$C_{14}H_{10}O_4$	5.32	241.0495	241.0493	−0.774	211.00470
Cinnamic acid*	$C_9H_8O_2$	5.39	147.0441	147.0445	−0.074	102.94863, 129.04442
Enterodiol-*O*-glucuronide	$C_{24}H_{30}O_{10}$	6.79	477.1755	477.1774	1.298	175.02505, 301.12904, 459.15735

* Compounds identified by comparing with the respective standard.

their metabolites. Only one lignan and one flavonoid metabolite were detected. As depicted in Table 2, 80 % of the metabolites resulted from phase II reactions, while the remaining 20 % were a result of phase I reactions. Moreover, 11 compounds identified are parent compounds and the remaining correspond to their metabolites. Considering the phenolic compounds previously reported in the CSS extract (Pinto, Vieira, et al., 2021), metabolites from pyrogallol, gallic, protocatechuic and ellagic acids were identified in the blood serum. Pyrogallol, a gallic acid metabolite produced by decarboxylation, was probably formed during extraction of CSS under high temperature (220 °C). All pyrogallol metabolites resulted from phase II reactions, namely (di)methylation, glucuronidation and sulfation. Protocatechuic acid, also found in the CSS extract, is a catechin metabolite formed via thermal decomposition (Pinto, Vieira, et al., 2021). Like drugs, some phenolic compounds may not undergo phase I reactions and can be directly deactivated by phase II reactions (Pimpão et al., 2015). This is the case of protocatechuic acid. Unmetabolized protocatechuic acid and three phase II metabolites were detected. A fraction of ellagic acid, belonging to hydrolysable tannins class derived from gallic acid, also reached the systemic circulation unchanged. Nevertheless, dimethyl-ellagic acid was also identified, as well as urolithin A metabolites, including sulfated and methylated forms. Urolithins are gut microbiota metabolites of ellagitannins and ellagic acid (Tu, Li, & Zhou, 2021). Even though chestnut shells are rich in ellagitannins, the SWE extraction at 220 °C led to the degradation of ellagitannins to ellagic acid, which is present in the CSS extract (Pinto, Cádiz-Gurrea, Vallverdú-Queralt, et al., 2021; Pinto, Vieira, et al., 2021). Furthermore, gallic acid only underwent hydrogenation forming dihydrogallic acid, a phase I metabolite also found in rice bran (Bhat

et al., 2020). Likewise, gallic acid, pyrogallol, ellagic acid, methylellagic acid and urolithins and their methylated, sulfated and glucuronidated metabolites were detected in plasma, bile, liver, and intestine from rats orally administered with 150 mg/kg b.w. *Sanguisorba officinalis* tannins (Tu et al., 2021).

Regarding the novel phenolic compounds identified in the CSS extract, CA and FA underwent phase I (hydrogenation and hydroxylation) and II reactions (methylation, sulfation and glucuronidation). Beyond phenolic compounds that escape first-pass metabolism, phase I metabolites may also experience other biotransformations, namely glucuronidation, sulfation and methylation (López-Yerena, Domínguez-López, et al., 2021). In this scenario, hydrogenated metabolites of CA and FA were further conjugated with glucuronic acid, sulfonate, and methyl groups. Additionally, CA and FA were also directly metabolized by phase II enzymes producing sulfated and methylated plus sulfated or glucuronidated metabolites. Otherwise, hydroxyferulic acid was formed via hydroxylation of FA by ferulate hydroxylase, acting as precursor in the biosynthesis of sinapic acid (López-Yerena, Domínguez-López, et al., 2021). Hydroxychlorogenic acid was the only chlorogenic acid metabolite identified, while unmetabolized *ρ*-coumaric and *m*-coumaric acids reached the systemic circulation along with the phase II metabolite methyl-coumaric acid-*O*-sulfate. Shi et al. (2019) described an identical plasma metabolomic profile of CA orally administered to rats, reporting benzoic, *m*-coumaric, DHCA, hydroxyhippuric acid, HPPA and vanillic acid, as well as CA, FA and DHFA and their sulfated and glucuronidated forms. Considering hydroxybenzoic acids, syringic acid and three conjugates, as well as 3-HBA and its sulfated form, were present. HBA may have resulted from the degradation of more complex hydroxybenzoic acids, such as gallic, protocatechuic, dihydroxybenzoic and syringic acids via dehydroxylation and decarboxylation (Shi et al., 2019). Likewise, the hippuric acid detected derives from benzoic acid formed by the degradation of other phenolic compounds and then conjugated with glycine (López-Yerena, Domínguez-López, et al., 2021). Furthermore, unmetabolized HPPA, a flavonoid or phenolic acid metabolite produced by the gut microbiota, was identified along with two phase II metabolites. According to Konishi and Kobayashi (2004), HPPA is a major CA metabolite being able to permeate intestinal Caco-2 cells. Only two hydroxyphenylacetic acid metabolites derived from sulfation and glucuronidation reached the blood.

In contrast to the CSS extract, (*epi*)catechin gallate, (*epi*)gallocatechin and (*epi*)gallocatechin gallate were not detected in blood serum owing to their poor absorption and high excretion rates. Only one catechin metabolite was found in serum, namely (*epi*)catechin-*O*-sulfate. Besides, protocatechuic acid, HPPA, 3-hydroxyphenylacetic acid and benzoic acid and derivatives may also be catechin metabolites (Shang et al., 2017).

Furthermore, secoisolariciresinol was the only lignan identified along with two gut microbial metabolites, namely enterodiol-*O*-glucuronide and enterolactone-*O*-disulfate. Catechol, a microbial metabolite, was also found along with its sulfated, methylated and glucuronidated conjugates. In another study, the metabolomic profile of Chinese water chestnut also revealed CA, chlorogenic, cinnamic, and phenylacetic acids (Li, Pan, He, Yuan, & Li, 2016).

Most of the phenolic acids identified are weak basic molecules with low molecular weight (<250 g/mol) and moderate lipophilicity (logP ~ 0.9) which encourages their absorption by passive transport (López-Yerena, Domínguez-López, et al., 2021; Pimpão et al., 2015). The detection of these compounds in serum proved their absorption in unmetabolized form. Additionally, phase II metabolites were secreted into circulating blood by transporters, owing to their high polarity and molecular weight.

3.5.2. Quantification of phenolic compounds and metabolites

Although it was not possible to quantify most of the metabolites due to their extremely low concentrations, some phenolic compounds and metabolites were quantified as shown in Table 3.

Table 3
Quantification of phenolic compounds metabolites in blood serum from rats treated with distilled water (control group), 50 mg/kg b.w. and 100 mg/kg b.w. of *C. sativa* shells extract analysed by LC-ESI-LTQ-Orbitrap-MS.

Phenolic compounds and metabolites	Concentration (nmol/mL blood serum)		
	Control (water)	CSS extract 50 mg/kg b.w.	CSS extract 100 mg/kg b.w.
Phenolic acids – Hydroxybenzoic acids			
3-Hydroxybenzoic acid	n.i.	205.86 ± 48.29^{a}	163.36 ± 31.16^{b}
Protocatechuic acid	n.i.	1.69 ± 0.45^{a}	0.86 ± 0.25^{b}
Dihydrogallic acid	n.i.	1.76 ± 0.46^{a}	1.55 ± 0.41^{a}
Syringic acid	n.i.	3.24 ± 1.05^{a}	2.72 ± 0.80^{a}
Hippuric acid	7.20 ± 1.43^{b}	13.19 ± 2.02^{a}	13.43 ± 2.75^{a}
Phenolic acids – Hydroxycinnamic acids			
Caffeic acid-*O*-sulfate	n.i.	0.15 ± 0.02^{a}	0.13 ± 0.02^{b}
Dihydrocaffeic acid	n.i.	1.95 ± 0.29^{a}	1.78 ± 0.40^{a}
Dihydrocaffeic acid-*O*-sulfate	n.i.	0.93 ± 0.16^{a}	0.97 ± 0.19^{a}
Dihydrocaffeic acid-*O*-glucuronide	n.i.	0.04 ± 0.01^{a}	0.04 ± 0.01^{a}
Methyl-ferulic acid-*O*-sulfate	n.i.	0.44 ± 0.08^{a}	0.36 ± 0.05^{b}
Dihydroferulic acid-*O*-sulfate	n.i.	2.38 ± 0.38^{a}	2.49 ± 0.51^{a}
Dihydroferulic acid-*O*-glucuronide	n.i.	0.24 ± 0.07^{b}	0.32 ± 0.12^{a}
p-Coumaric acid	n.i.	0.26 ± 0.04^{a}	0.23 ± 0.03^{b}
Phenolic acids - Hydroxyphenylpropanoic acids			
Hydroxyphenylpropionic acid	n.i.	318.79 ± 63.15^{a}	333.80 ± 60.37^{a}
Hydroxyphenylpropionic acid-*O*-sulfate	n.i.	225.13 ± 60.59^{a}	219.54 ± 65.34^{a}
Flavonoids			
(*Epi*)catechin-*O*-sulfate	n.i.	1.32 ± 0.40^{b}	1.51 ± 0.10^{a}
Lignans			
Secoisolariciresinol	n.i.	0.33 ± 0.08^{a}	0.34 ± 0.07^{a}
Other polyphenols- Hydroxycoumarins			
Methyl-urolithin A	n.i.	0.22 ± 0.05^{b}	0.26 ± 0.06^{a}
Other polyphenols			
Catechol-*O*-sulfate	n.i.	3.50 ± 0.47^{a}	3.42 ± 0.42^{a}
Catechol-*O*-glucuronide	n.i.	0.12 ± 0.03^{b}	0.15 ± 0.04^{a}
Methyl-catechol-*O*-sulfate	n.i.	0.87 ± 0.18^{b}	1.04 ± 0.17^{a}

n.i., non-identified. Results are expressed as mean ± standard deviation, $n = 6$ in each group. Different letters (a and b) in the same line indicate significant differences between groups ($p < 0.05$).

The major phenolic compounds were HPPA (318.79 and 333.80 nmol/mL for 50 and 100 mg/kg b.w., respectively), followed by 3-HBA (205.86 and 163.36 nmol/mL, respectively), while HPPA-*O*-sulfate was the main metabolite (225.13 and 219.54 nmol/mL).

Among hydroxybenzoic acids, protocatechuic, syringic and hippuric acids were also present in considerable amounts, while only one metabolite resulting from the hydrogenation of gallic acid was quantified. Hippuric acid was the only compound quantified in the control group, but in trace levels ($p < 0.05$) compared to the treatment groups. Hippuric acid is an endogenous metabolite detected after the consumption of foods containing polyphenols, such as whole grains, cereals, and vegetable oils, which may explain its presence in control group. All animals were fed standard pellet diet that is composed of corn starch, soybean oil, minerals, vitamins, and others (e.g., amino acids and polysaccharides) (National Research Council (US) Subcommittee on

Laboratory Animal Nutrition, 1995). Some of these ingredients, such as corn starch and soybean oil, derived from cereals and plants rich in polyphenols, namely hydroxybenzoic (such as gallic and protocatechuic acids) and hydroxycinnamic acids (namely CA, FA, chlorogenic, coumaric and vanillic acids) (Luzardo-Ocampo et al., 2017). Therefore, the trace levels of hippuric acid in rats may result from the metabolization of hydroxybenzoic acids, present in the cereals and vegetable oil derived ingredients, into benzoic acid by phase I enzymes, and further conjugation with glycine (endogenously produced from other amino acids delivered by diet).

Considering hydroxycinnamic acids, metabolites of CA and FA arising from phase I and II reactions were present in both treatment groups, as well as ρ-coumaric acid. CA metabolites represent 2.92–3.07 nmol/mL, while 3.06–3.17 nmol/mL correspond to FA metabolites.

Only one flavonoid metabolite, namely (*epi*)catechin-*O*-sulfate, and one ellagic acid metabolite, namely methyl-urolithin A, were present in traceable amounts. Low amounts of secoisolariciresinol were also detected, without significant differences ($p > 0.05$). Phase II metabolites of catechol were determined in the following decreasing order: catechol-*O*-sulfate > methyl-catechol-*O*-sulfate > catechol-*O*-glucuronide.

As can be observed in Table 3, five compounds (namely 3-HBA, protocatechuic acid, CA-*O*-sulfate, methyl-FA-*O*-sulfate, and ρ-coumaric acid) achieved the highest concentrations in the 50 mg/kg b.w. CSS extract group ($p < 0.05$), while higher concentrations ($p < 0.05$) of DHFA-*O*-glucuronide, (*epi*)catechin-*O*-sulfate, methyl-urolithin A, catechol-*O*-glucuronide, and methyl-catechol-*O*-sulfate were detected in the 100 mg/kg b.w. CSS extract group. According to Hussain, Hassan, Waheed, Javed, Farooq, and Tahir (2019), phenolic compounds are absorbed by passive diffusion or through carriers located in the intestine and expressed in the cell membranes, including *P*-glycoprotein and cotransporters for SGLT1. Therefore, these differences may be due to the saturation of these carriers with other compounds that difficult their transport through intestinal barrier and absorption.

As shown in Table 3, there was no direct proportionality between the concentration of phenolic compounds and their metabolites and the increase of extract dose from 50 to 100 mg/kg b.w. These differences may be explained by the poor reproducibility in the experimental animal research due to the high heterogenization of responses and biological variation (Voelkl et al., 2020). As stated by previous studies, the efficacy of a treatment depends not only of its nature, duration, and intensity, but also of the phenotype of the animals involving internal state (defined by genotype and previous experiences) and external factors (such as the environment) that affect morphological, physiological and behavioral traits (López-Yerena, Perez, Vallverdú-Queralt, & Escribano-Ferrer, 2020; Voelkl et al., 2020). Another reason for these differences is related to the metabolomic technology selected and the sample pre-treatment that may affect the sensitivity, selectivity, and reproducibility of the analytical procedure and, consequently, the identification and quantification of the phenolic compounds and their metabolites (López-Yerena, Domínguez-López, et al., 2021). The sample pre-treatment aims to: i) minimize the interferences of undesired endogenous compounds in the extracted samples; ii) improve the selectivity of targeted analytes; iii) enhance the sample pre-concentration to improve sensitivity; and iv) stabilize the sample using an inert solvent (López-Yerena, Domínguez-López, et al., 2021). Blood serum contains proteins, glucose, minerals, and blood cells that may interfere with the detection of the targeted analytes (López-Yerena et al., 2020). Phenolic compounds and their metabolites may have a high binding affinity to plasma proteins and other cellular components, such as phospholipids, which highlights the need of a sample pre-treatment to remove these substances from serum, reducing the potential matrix effects and the ion suppression phenomena (López-Yerena et al., 2020). Although the protein precipitation is a simple and fast procedure to eliminate these interferences, previous studies suggest that it may not deliver an entirely clean extract (López-Yerena, Domínguez-López, et al., 2021; López-Yerena et al., 2020). Additionally, other difficulties in the sample clean-up include metabolite degradation owing to multi-step procedures for sample preparation, instability of compounds, and low analyte concentration (López-Yerena, Domínguez-López, et al., 2021).

In summary, the main phenolic compounds identified in serum were 3-HBA, HPPA and HPPA-*O*-sulfate, with concentrations beyond 200 nmol/mL blood serum, representing almost 96 % of the total phenolic content. In general, similar concentrations of phenolic compounds and their metabolites were detected in both CSS extract groups, pointing out identical metabolomic profiles and correlating with similar *in-vivo* antioxidant effects attested in both groups.

3.6. Histological evaluation of liver and kidney

The safety of CSS extract for daily intake should be attested prior to its use as nutraceutical. Recently, Pinto, Vieira, et al. (2021) proved the safety of the CSS extract in intestinal cells (Caco-2 and HT29-MTX) up to 1000 μg/mL. In this study, hematoxylin and eosin staining were used to evaluate the integrity and morphology of liver and kidney tissues (Fig. 2).

Hematoxylin stains acidic structures (e.g., nucleus containing nucleic acids) in purple, whereas eosin stains basic structures (e.g., cytoplasm and extracellular containing proteins) in pink. As shown in Fig. 2, the liver morphology and integrity of control, vitamin C and CSS extract groups are similar, maintaining an intact and homogeneous tissue architecture without structural changes or histopathological signs. Likewise, no significant changes were observed in kidney tissues among control and CSS extract groups at both doses, revealing normal cytology and renal parenchymal structure devoid of any pathological features and toxicity signs induced by the intake of CSS extract. Moreover, liver and kidney tissues are characterized by the lack of derangement, necrosis, inflammation signs or other pathological features typically present in most metabolic pathologies. The morphology and barrier integrity of liver and kidney tissues remained unchanged after the oral treatment with CSS extract, demonstrating an apparent resemblance compared to the control. Overall, the results suggested the safety of the CSS extract for liver and kidney up to 100 mg/kg b.w. due to the maintenance of cell membrane integrity, without signs of membrane disruption and leakage of cytoplasmic and nuclear content. As a future perspective, a more in-depth study of the toxicity of chestnut shells extract in a long-term intake, on different organs and body fluids, could be beneficial to understand the effects of CSS in a daily-basis consumption as a nutraceutical.

3.7. Principal component analysis

PCA is a useful multivariate statistical tool for data analysis, enabling a reduction of data dimensionality to explore unsupervised patterns in a set of samples. Fig. 3 represents a scores plot of treatment groups and a biplot diagram of variables regarding *in-vivo* antioxidant activity and metabolomic analysis in blood serum. This analysis will allow to ascertain if the two doses of the CSS extract tested achieved considerable differences in the *in-vivo* antioxidant responses and metabolomic profiles, as well as to comprehend the main phenolic compounds and metabolites that contributed to the antioxidant enzymes' activities and prevention of LPO in each group.

The score plot showed a clear separation of 50 and 100 mg/kg b.w. CSS extract groups, with 39.67 % of explained cumulative variance (Fig. 3A), indicating a strong effect of the metabolomic profiling on the *in-vivo* antioxidant activity of blood serum. The PC 1 is the main component responsible for clustering separately the two treatment groups with 21.87 % of explained variance, highlighting substantially different *in-vivo* antioxidant responses for 50 and 100 mg/kg b.w. CSS extract groups owing to the clear separation of the two clusters. Considering the position in a two-dimensional space, the variables closest and farthest from the diagram origin are positively correlated, while a negative correlation is suggested for variables placed oppositely

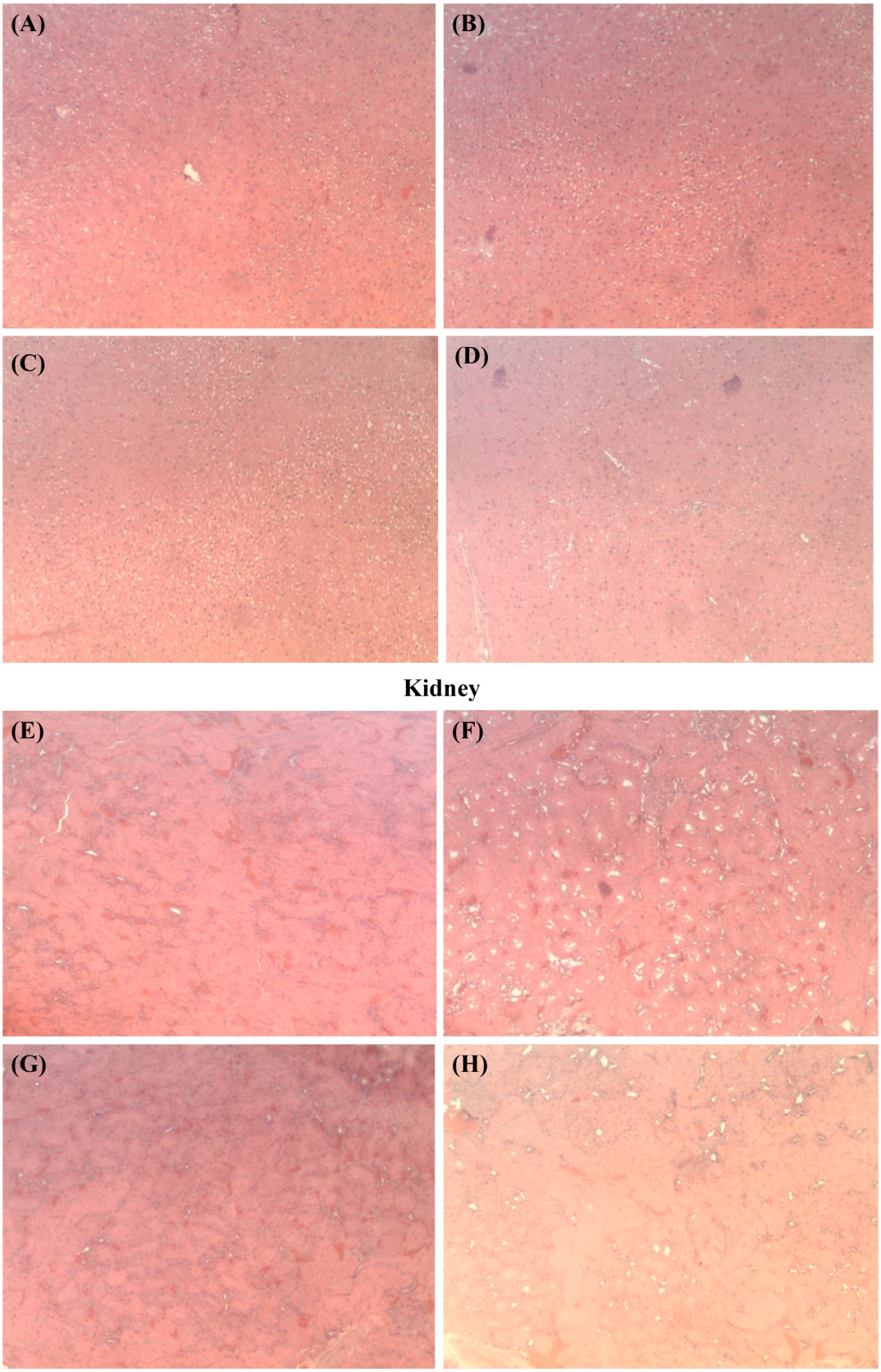

Fig. 2. Histology examination of liver and kidney tissues sections prepared by hematoxylin and eosin staining and observed at 10x magnification. Figures A–D correspond to liver sections: (A) CSS 50 mg/kg b.w., (B) CSS 100 mg/kg b.w., (C) Vitamin C 50 mg/kg b.w., and (D) Control group. Figures E-H correspond to kidney sections: (E) CSS 50 mg/kg b.w., (F) CSS 100 mg/kg b.w., (G) Vitamin C 50 mg/kg b.w., and (H) Control group.

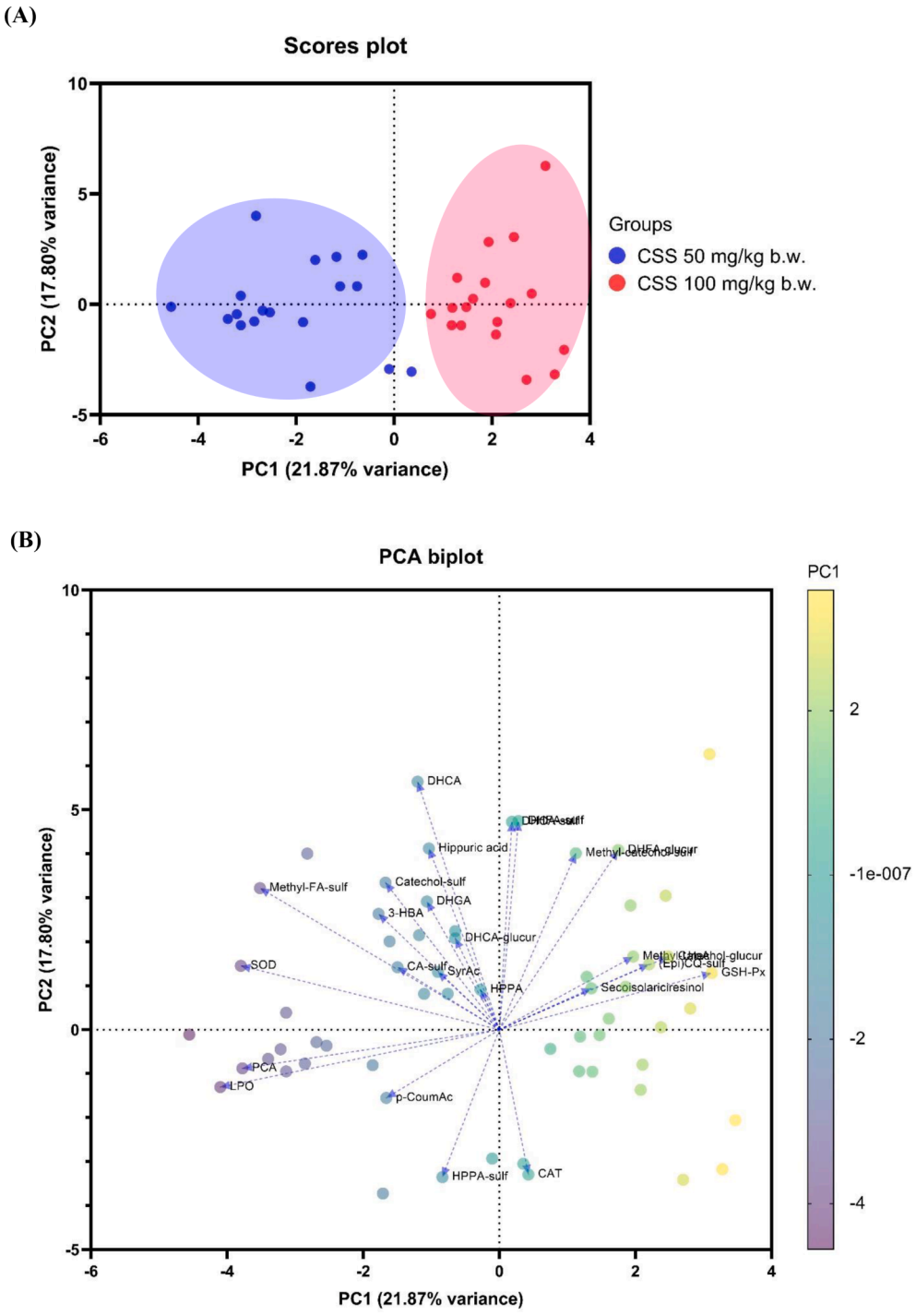

Fig. 3. Principal component analysis on the antioxidant enzymes activities and metabolomic profile of blood serum from rats treated with CSS extract at 50 and 100 mg/kg b.w. (A) Scores plot of treatment groups and (B) Biplot of variables. CA, caffeic acid. CAT, catalase activity. DHCA, dihydrocaffeic acid. DHFA, dihydroferulic acid. DHGA, dihydrogallic acid. (*Epi*)CQ, (*epi*)catechin. FA, ferulic acid. glucur, glucuronide. GSH-Px, glutathione peroxidase activity. 3-HBA, 3-hydroxybenzoic acid. HPPA, hydroxyphenylpropionic acid. LPO, lipid peroxidation. *ρ*-CoumAc, *ρ*-Coumaric acid. PCA, protocatechuic acid. SOD, superoxide dismutase activity. sulf, sulfate. SyrAc, syringic acid.

in the plot. As depicted in Fig. 3B, the biplot diagram suggests that the *in-vivo* antioxidant activity of the 100 mg/kg b.w. CSS extract group (colored green and yellow) is mainly ascribed to the variable GSH-Px and contents of catechol-*O*-glucuronide, DHFA-*O*-glucuronide, (*epi*)catechin-*O*-sulfate, methyl-catechol-*O*-sulfate, methyl-urolithin A, and secoisolariciresinol. Considering the lowest dose treatment group (marked in blue and purple in the diagram), the variables SOD, LPO and contents of CA-*O*-sulfate, *ρ*-coumaric acid, catechol-*O*-sulfate, DHCA, DHCA-*O*-glucuronide, dihydrogallic acid, 3-HBA, hippuric acid, HPPA, HPPA-*O*-sulfate, methyl-FA-*O*-sulfate, protocatechuic acid and syringic acid are strongly correlated with the *in-vivo* antioxidant activity of 50 mg/kg b.w. CSS extract group. Overall, the *in-vivo* antioxidant activity of the 50 mg/kg b.w. CSS extract group is closely related to the SOD activity and the prevention of LPO, which are probably due to the phenolic acids and metabolites, mainly hydroxybenzoic and hydroxycinnamic acids. Notwithstanding, the GSH-Px activity is the main parameter contributing to the *in-vivo* antioxidant response of the 100 mg/kg b.w. CSS extract group, mostly attributed to the lignan and metabolites of catechol, (*epi*)catechin and DHFA. Additionally, the CAT activity did not seem to contribute with a significant effect for any of the treatment groups.

4. Conclusion

Through this work, a nutraceutical extract from chestnut shells recovered by an emerging green technology was exploited as a prominent source of antioxidant compounds, embracing *in-vivo* health-promoting effects. Even though the European legislation applied to the validation of new nutraceuticals remains vague, a deep understanding of the *in-vitro* and *in-vivo* biological effects should be guaranteed prior to its use as functional ingredient. This is the first study that validated a novel nutraceutical ingredient extracted from CSS by *in-vivo* assays in compliance with the European Directive 2010/63/EU for animal studies. Protective effects against oxidative stress-mediated damages were revealed in liver, kidney, and blood by upmodulating antioxidant enzymes' activities and downregulating lipid peroxidation, with slightly better antioxidant responses *in-vivo* for 100 mg/kg b.w. CSS extract group along with mild hypoglycemic and hypolipidemic effects (suggesting a forthcoming exploitation of CSS as a preventive measure against metabolic disorders). Likewise, the metabolomic profile was useful for the fingerprinting of phenolic compounds and metabolites in blood serum, indicating identical profiling for both doses and correlating them with similar *in-vivo* bioactivity. Unmetabolized phenolic compounds and their phase I (hydrogenation and hydroxylation) and phase II metabolites (sulfation, methylation and glucuronidation) were seen. Hence, 100 mg/kg b.w. of CSS extract may be selected to use as a nutraceutical active ingredient in future studies. The *in-vivo* studies using the animal models confirmed the results accomplished on the *in-vitro* assays previously published, proposing a new strategy for the industrial valorization of chestnut shells as a promissory and appealing source of anti-aging compounds for nutraceuticals. The next step will be centered on design a sustainable nutraceutical industrial scalable product incorporating the CSS extract as active ingredient.

CRediT authorship contribution statement

Diana Pinto: Methodology, Software, Formal analysis, Investigation, Writing – original draft. **Andreia Almeida:** Methodology, Formal analysis, Investigation, Writing – review & editing. **Anallely López-Yerena:** Methodology, Formal analysis, Investigation, Writing – review & editing. **Soraia Pinto:** Methodology, Formal analysis, Investigation. **Bruno Sarmento:** Methodology, Funding acquisition, Resources. **Rosa Lamuela-Raventós:** Methodology, Funding acquisition, Resources. **Anna Vallverdú-Queralt:** Methodology, Supervision, Writing – review & editing. **Cristina Delerue-Matos:** Methodology, Supervision, Resources. **Francisca Rodrigues:** Methodology, Conceptualization, Validation, Investigation, Resources, Writing – review & editing, Supervision, Project administration, Funding acquisition.

Declaration of Competing Interest

The authors declare that they have no known competing financial interests or personal relationships that could have appeared to influence the work reported in this paper.

Data availability

The authors do not have permission to share data.

Acknowledgements

The authors' kindly thanks to Sortegel (Sortes, Portugal) for the samples. This work received financial support from national funds (UIDB/50006/2020), project PTDC/ASP-AGR/29277/2017 - *Castanea sativa* shells as a new source of active ingredients for Functional Food and Cosmetic applications: a sustainable approach, and project 5537 DRI, Sérvia 2020/21 from Portuguese-Serbia Bilateral Cooperation - Development of functional foods incorporating a chestnut shells extract obtained by subcritical water, supported by national funds by FCT / MCTES and co-supported by Fundo Europeu de Desenvolvimento Regional (FEDER) throughout COMPETE 2020 - Programa Operacional Competitividade e Internacionalização (POCI-01-0145-FEDER-029277). Diana Pinto (SFRH/BD/144534/2019) and Soraia Pinto (SFRH/BD/144719/2019) are thankful for their PhD grants financed by FCT/MCTES and POPH-QREN and supported by funds from European Union (EU) and Fundo Social Europeu (FSE) through Programa Operacional Regional Norte. Francisca Rodrigues is grateful for her contract (CEECIND/01886/2020) financed by FCT/MCTES—CEEC Individual 2020 Program Contract. Anna Vallverdú-Queralt thanks the Spanish Ministerio de Ciencia, Innovación y Universidades for the Ramon y Cajal contract (RYC-2016-19355).

Appendix A. Supplementary data

Supplementary data to this article can be found online at https://doi.org/10.1016/j.foodchem.2022.134546.

References

Babbar, N., Oberoi, H. S., & Sandhu, S. K. (2015). Therapeutic and nutraceutical potential of bioactive compounds extracted from fruit residues. *Critical Reviews in Food Science and Nutrition, 55*, 319–337. https://doi.org/10.1080/10408398.2011.653734

Barreira, J. C. M., Ferreira, I. C. F. R., Oliveira, M. B. P. P., & Pereira, J. A. (2008). Antioxidant activities of the extracts from chestnut flower, leaf, skins and fruit. *Food Chemistry, 107*, 1106–1113. https://doi.org/10.1016/j.foodchem.2007.09.030

Bhat, F. M., Sommano, S. R., Riar, C. S., Seesuriyachan, P., Chaiyaso, T., & Prom-u-Thai, C. (2020). Status of bioactive compounds from bran of pigmented traditional rice varieties and their scope in production of medicinal food with nutraceutical importance. *Agronomy, 10*, 1817. https://www.mdpi.com/2073-4395/10/11/1817.

Escobar-Avello, D., Mardones, C., Saéz, V., Riquelme, S., von Baer, D., Lamuela-Raventós, R. M., & Vallverdú-Queralt, A. (2021). Pilot-plant scale extraction of phenolic compounds from grape canes: Comprehensive characterization by LC-ESI-LTQ-Orbitrap-MS. *Food Research International, 143*, Article 110265. https://doi.org/10.1016/j.foodres.2021.110265

Eseberri, I., Trepiana, J., Léniz, A., Gómez-García, I., Carr-Ugarte, H., González, M., & Portillo, M. P. (2022). Variability in the beneficial effects of phenolic compounds: A review. *Nutrients, 14*, 1925. https://doi.org/10.3390/nu14091925

Hong, M. Y., Groven, S., Marx, A., Rasmussen, C., & Beidler, J. (2018). Anti-inflammatory, antioxidant, and hypolipidemic effects of mixed nuts in atherogenic diet-fed rats. *Molecules, 23*, 3126. https://doi.org/10.3390/molecules23123126

Hussain, M. B., Hassan, S., Waheed, M., Javed, A., Farooq, M. A. , & Tahir, A. (2019). Bioavailability and metabolic pathway of phenolic compounds. In M. Soto-Hernández, R. García-Mateos, & M. Palma-Tenango (Eds.), *Plant physiological aspects of phenolic compounds*. IntechOpen. doi:10.5772/intechopen.84745.

Kimura, H., Ogawa, S., Sugiyama, A., Jisaka, M., Takeuchi, T., & Yokota, K. (2011). Anti-obesity effects of highly polymeric proanthocyanidins from seed shells of Japanese horse chestnut (*Aesculus turbinata* Blume). *Food Research International, 44*, 121–126. https://doi.org/10.1016/j.foodres.2010.10.052

Konishi, Y., & Kobayashi, S. (2004). Microbial metabolites of ingested caffeic acid are absorbed by the monocarboxylic acid transporter (MCT) in intestinal Caco-2 cell monolayers. *Journal of Agricultural and Food Chemistry, 52*, 6418–6424. https://doi.org/10.1021/jf049560y

Lee, S. R., Jo, S. L., Heo, J. H., Kim, T.-W., Lee, K.-P., & Hong, E.-J. (2022). The aqueous fraction of *Castanea crenata* inner shell extract reduces obesity and intramuscular lipid accumulation via induction of mitochondrial respiration and fatty acid oxidation in muscle. *Phytomedicine, 98*, Article 153974. https://doi.org/10.1016/j.phymed.2022.153974

Li, Y. X., Pan, Y. G., He, F. P., Yuan, M. Q., & Li, S. B. (2016). Pathway analysis and metabolites identification by metabolomics of etiolation substrate from fresh-cut Chinese water chestnut (*Eleocharis tuberosa*). *Molecules, 21*, 1648. https://doi.org/10.3390/molecules21121648

Liu, X., Wang, H., Liang, X., & Roberts, M. S. (2017). Hepatic metabolism in liver health and disease. In P. Muriel (Ed.), *Liver Pathophysiology* (pp. 391–400). Academic Press. https://doi.org/10.1016/B978-0-12-804274-8.00030-8.

López-Yerena, A., Domínguez-López, I., Vallverdú-Queralt, A., Pérez, M., Jáuregui, O., Escribano-Ferrer, E., & Lamuela-Raventós, R. M. (2021). Metabolomics technologies for the identification and quantification of dietary phenolic compound metabolites: An overview. *Antioxidants, 10*, 846. https://doi.org/10.3390/antiox10060846

López-Yerena, A., Perez, M., Vallverdú-Queralt, A., & Escribano-Ferrer, E. (2020). Insights into the binding of dietary phenolic compounds to human serum albumin and food-drug interactions. *Pharmaceutics, 12*, 1123. https://doi.org/10.3390/pharmaceutics12111123

López-Yerena, A., Vallverdú-Queralt, A., Jáuregui, O., Garcia-Sala, X., Lamuela-Raventós, R. M., & Escribano-Ferrer, E. (2021). Tissue distribution of oleocanthal and its metabolites after oral ingestion in rats. *Antioxidants, 10*, 688. https://www.mdpi.com/2076-3921/10/5/688.

Luzardo-Ocampo, I., Campos-Vega, R., Gaytán-Martínez, M., Preciado-Ortiz, R., Mendoza, S., & Loarca-Piña, G. (2017). Bioaccessibility and antioxidant activity of free phenolic compounds and oligosaccharides from corn (*Zea mays* L.) and common bean (*Phaseolus vulgaris* L.) chips during *in vitro* gastrointestinal digestion and simulated colonic fermentation. *Food Research International, 100*, 304–311. https://doi.org/10.1016/j.foodres.2017.07.018

Marhuenda-Muñoz, M., Laveriano-Santos, E. P., Tresserra-Rimbau, A., Lamuela-Raventós, R. M., Martínez-Huélamo, M., & Vallverdú-Queralt, A. (2019). Microbial phenolic metabolites: Which molecules actually have an effect on human health? *Nutrients, 11*, 2725. https://www.mdpi.com/2072-6643/11/11/2725.

Martins, N., Barros, L., & Ferreira, I. C. F. R. (2016). *In vivo* antioxidant activity of phenolic compounds: Facts and gaps. *Trends in Food Science & Technology, 48*, 1–12. https://doi.org/10.1016/j.tifs.2015.11.008

National Research Council (US) Subcommittee on Laboratory Animal Nutrition. (1995). *Nutrient requirements of laboratory animals* (4th ed.). Washington (DC): National Academies Press (Chapter 2). Available from https://www.ncbi.nlm.nih.gov/books/NBK231925/.

Noh, J.-R., Gang, G.-T., Kim, Y.-H., Yang, K.-J., Hwang, J.-H., Lee, H.-S., … Lee, C.-H. (2010). Antioxidant effects of the chestnut (*Castanea crenata*) inner shell extract in *t*-BHP-treated HepG2 cells, and CCl4- and high-fat diet-treated mice. *Food and Chemical Toxicology, 48*, 3177–3183. https://doi.org/10.1016/j.fct.2010.08.018

Noh, J. R., Kim, Y. H., Gang, G. T., Hwang, J. H., Lee, H. S., Ly, S. Y., … Lee, C. H. (2011). Hepatoprotective effects of chestnut (*Castanea crenata*) inner shell extract against chronic ethanol-induced oxidative stress in C57BL/6 mice. *Food and Chemical Toxicology, 49*, 1537–1543. https://doi.org/10.1016/j.fct.2011.03.045

Orrego-Lagarón, N., Martínez-Huélamo, M., Vallverdú-Queralt, A., Lamuela-Raventos, R. M., & Escribano-Ferrer, E. (2015). High gastrointestinal permeability and local metabolism of naringenin: Influence of antibiotic treatment on absorption and metabolism. *British Journal of Nutrition, 114*, 169–180. https://doi.org/10.1017/S0007114515001671

Pimpão, R. C., Ventura, M. R., Ferreira, R. B., Williamson, G., & Santos, C. N. (2015). Phenolic sulfates as new and highly abundant metabolites in human plasma after ingestion of a mixed berry fruit purée. *British Journal of Nutrition, 113*, 454–463. https://doi.org/10.1017/s0007114514003511

Pinto, D., Cádiz-Gurrea, M.d.l. L., Sut, S., Ferreira, A. S., Leyva-Jimenez, F. J., Dall'Acqua, S., … Rodrigues, F. (2020). Valorisation of underexploited *Castanea sativa* shells bioactive compounds recovered by supercritical fluid extraction with CO_2: A response surface methodology approach. *Journal of CO2 Utilization, 40*, Article 101194. https://doi.org/10.1016/j.jcou.2020.101194

Pinto, D., Cádiz-Gurrea, M.d.l. L., Vallverdú-Queralt, A., Delerue-Matos, C., & Rodrigues, F. (2021). *Castanea sativa* shells: A review on phytochemical composition, bioactivity and waste management approaches for industrial valorization. *Food Research International, 144*, Article 110364. https://doi.org/10.1016/j.foodres.2021.110364

Pinto, D., Cádiz-Gurrea, M. d. l. L., Garcia, J., Saavedra, M. J., Freitas, V., Costa, P., … Rodrigues, F. (2021). From soil to cosmetic industry: Validation of a new cosmetic ingredient extracted from chestnut shells. *Sustainable Materials and Technologies*, *29*, Article e00309. doi:10.1016/j.susmat.2021.e00309.

Pinto, D., Silva, A. M., Freitas, V., Vallverdú-Queralt, A., Delerue-Matos, C., & Rodrigues, F. (2021). Microwave-assisted extraction as a green technology approach to recover polyphenols from *Castanea sativa* shells. *ACS Food Science & Technology, 1*, 229–241. https://doi.org/10.1021/acsfoodscitech.0c00055

Pinto, D., Vieira, E. F., Peixoto, A. F., Freire, C., Freitas, V., Costa, P., … Rodrigues, F. (2021). Optimizing the extraction of phenolic antioxidants from chestnut shells by subcritical water extraction using response surface methodology. *Food Chemistry, 334*, Article 127521. https://doi.org/10.1016/j.foodchem.2020.127521

Sangiovanni, E., Piazza, S., Vrhovsek, U., Fumagalli, M., Khalilpour, S., Masuero, D., … Dell'Agli, M. (2018). A bio-guided approach for the development of a chestnut-based proanthocyanidin-enriched nutraceutical with potential anti-gastritis properties. *Pharmacological Research, 134*, 145–155. https://doi.org/10.1016/j.phrs.2018.06.016

Sasot, G., Martínez-Huélamo, M., Vallverdú-Queralt, A., Mercader-Martí, M., Estruch, R., & Lamuela-Raventós, R. M. (2017). Identification of phenolic metabolites in human urine after the intake of a functional food made from grape extract by a high resolution LTQ-Orbitrap-MS approach. *Food Research International, 100*, 435–444. https://doi.org/10.1016/j.foodres.2017.01.020

Shang, Z., Wang, F., Dai, S., Lu, J., Wu, X., & Zhang, J. (2017). Profiling and identification of (-)-epicatechin metabolites in rats using ultra-high performance liquid chromatography coupled with linear trap-Orbitrap mass spectrometer. *Drug Testing and Analysis, 9*, 1224–1235. https://doi.org/10.1002/dta.2155

Shi, B., Yang, L., Gao, T., Ma, C., Li, Q., Nan, Y., … Zheng, X. (2019). Pharmacokinetic profile and metabolite identification of bornyl caffeate and caffeic acid in rats by high performance liquid chromatography coupled with mass spectrometry. *RSC Advances, 9*, 4015–4027. https://doi.org/10.1039/C8RA07972B

Sirtori, C. R., & Fumagalli, R. (2006). LDL-cholesterol lowering or HDL-cholesterol raising for cardiovascular prevention: A lesson from cholesterol turnover studies and others. *Atherosclerosis, 186*, 1–11. https://doi.org/10.1016/j.atherosclerosis.2005.10.024

Soussi, A., Gargouri, M., Akrouti, A., & El Feki, A. (2018). Antioxidant and nephro-protective effect of *Juglans regia* vegetable oil against lead-induced nephrotoxicity in rats and its characterization by GC-MS. *EXCLI Journal, 17*, 492–504. https://doi.org/10.17179/excli2018-1235

Su, X.-Y., Wang, Z.-Y., & Liu, J.-R. (2009). *In vitro* and *in vivo* antioxidant activity of *Pinus koraiensis* seed extract containing phenolic compounds. *Food Chemistry, 117*, 681–686. https://doi.org/10.1016/j.foodchem.2009.04.076

Tian, Z., & Liang, M. (2021). Renal metabolism and hypertension. *Nature Communications, 12*, 963. https://doi.org/10.1038/s41467-021-21301-5

Traber, M. G., & Stevens, J. F. (2011). Vitamins C and E: Beneficial effects from a mechanistic perspective. *Free Radical Biology and Medicine, 51*, 1000–1013. https://doi.org/10.1016/j.freeradbiomed.2011.05.017

Tsujita, T., Takaku, T., & Suzuki, T. (2008). Chestnut astringent skin extract, an alpha-amylase inhibitor, retards carbohydrate absorption in rats and humans. *Journal of Nutritional Science and Vitaminology, 54*, 82–88. https://doi.org/10.3177/jnsv.54.82

Tu, J., Li, Q., & Zhou, B. (2021). The tannins from *Sanguisorba officinalis* L. (Rosaceae): A systematic study on the metabolites of rats based on HPLC-LTQ-Orbitrap MS(2) analysis. *Molecules, 26*, 4053. https://doi.org/10.3390/molecules26134053

Voelkl, B., Altman, N. S., Forsman, A., Forstmeier, W., Gurevitch, J., Jaric, I., … Würbel, H. (2020). Reproducibility of animal research in light of biological variation. *Nature Reviews Neuroscience, 21*, 384–393. https://doi.org/10.1038/s41583-020-0313-3